Available online at www.sciencedirect.com
ScienceDirect
Journal of the European Ceramic Society 27 (2007) 1333–1337
www.elsevier.com/locate/jeurceramsoc

Tunnelling cracks in Al_2O_3/Al_2O_3–ZrO_2 layered composites

S. Beranič Klopčič, M. Ambrožič *, T. Kosmač, S. Novak

"Jožef Stefan" Institute, Jamova 39, Ljubljana, Slovenia

Available online 7 September 2006

Abstract

Two sizes of symmetrical, five-layered ceramic composites with alumina surface layers and alumina–zirconia inner layers were produced. Each composite had the same sequence and composition of individual layers; however, the measured strength of the large-sized sample was only 76 MPa to 115 MPa. This is due to the presence of tunnelling cracks that appear as a consequence of the tensile thermal residual stresses in the inner layers that develop during the cooling of the samples from the sintering temperature. The small-sized composite, with the slightly smaller layer thicknesses, had a higher strength: 317–378 MPa. The number and the position of the tunnelling cracks in the large-sized composite was not uniform through the depth of the sample, indicating the presence of crack splitting. The main reason for the different strengths of the small- and large-sized samples seems to be the different thicknesses of the innermost layers. Analytical calculations confirmed that tunnelling cracks can occur in the large-sized composite, providing that typical values of the material parameters from the literature are taken into account. According to these calculations, a thinner innermost layer in the large-sized composite would result in a crack-free material.

Keywords: Al_2O_3; ZrO_2; Composites; Defects; Strength

1. Introduction

Layered ceramic composites with compressive surface layers have received a lot of attention lately because of their superior mechanical properties. Frequently, alumina and zirconia, together or separately with other materials, were used to produce ceramics with compressive surface layers.[1–6] This kind of composite should have a higher strength and a higher toughness, but the problem of defects (as a consequence of residual stresses that are the result of having two materials with different thermal expansion coefficients), like tunnelling cracks, can occur. A composite with good mechanical properties can be prepared when the composite has a high surface-compressive stress. This can be achieved by having the appropriate thicknesses and composition.[7–9] Therefore, it is clear that the stress distribution in the composite has an important role. In addition to bulk stresses in such composites, macroscopic and microscopic stress fields in the boundary between the layers and between the alumina and alumina–zirconia grains, respectively, can be present, which affect the appearance of the cracks.[9] To avoid such defects, continuously or step-graded ceramics with many layers (with smaller compositional changes between neighbouring layers) are prepared. One of the methods for fabricating composites with compressive surface layers is slip-casting.[10] This is a relatively low-cost technique that can produce complex product shapes and a more complete dispersion of the powder in a relatively low-viscosity liquid. The disadvantages are lower production rates and a lower dimensional precision.

In this study we report on the fabrication of five-layered composites with two different sizes. The appearance of tunnelling cracks and their depth profiles in the composite were studied, and some analytical calculations of the marginal conditions for the appearance of cracks were made.

2. Experimental

The powders used in this study were alumina (A-16SG, Alcoa, USA, average particle size 0.7 μm, and specific surface area 6.3 m^2/g) and yttria partially stabilized zirconia (TZ-3Y, Tosoh, Japan, average particle size 0.3 μm, and specific surface area 16 m^2/g). The aqueous suspensions (75 wt.% of powder) were prepared by homogenizing the powders in an attritor mill with the addition of the deflocculant Dolapix CE-64 (Zschimmer & Schwarz, Germany). The homogeneous alumina (A) and alumina–zirconia suspensions with 20 wt.% (AZ0.8) and 40 wt.% (AZ0.6) of zirconia were used to form the alumina/alumina–zirconia layered composites. The sintered

* Corresponding author. Tel.: +386 1 477 39 40; fax: +386 1 251 93 85.
E-mail address: milan.ambrozic@ijs.si (M. Ambrožič).

0955-2219/$ – see front matter © 2006 Elsevier Ltd. All rights reserved.
doi:10.1016/j.jeurceramsoc.2006.08.001

compacts, with geometries 4.9 cm × 4.9 cm × 3.4 mm (large-sized sample) and 3.7 cm × 3.7 cm × 2.6 mm (small-sized sample), were prepared by casting the slurry into a porous mould made of plaster of paris. The symmetrical composites A/AZ0.8/AZ0.6/AZ0.8/A were made by casting one layer after another and drying the layers between castings so that the composition was not mixed during the processing. The composites were dried at room temperature and then sintered at 1550 °C for 2 h in air.

The ceramic plates were cut with a diamond saw to 3-mm wide bars (with the cutting direction perpendicular to the layers, as shown in Fig. 3), polished and observed with an optical microscope. The strength of the bars was measured using the four-point-bending method (20/10-mm span), the bending forces being perpendicular to the layers. For representative samples we measured the bending strength for both sides of the alumina layers as tensile layers; this was important to check because we could not expect the composites to be completely symmetrical.

3. Results and discussion

The layer compositions and the thicknesses of the small-sized and large-sized composite samples are presented in Table 1 and the corresponding material parameters are given in Table 2. The designations "top" and "bottom" indicate which of the alumina layers was exposed to the atmosphere and which was in contact with the porous mould during the slip-cast processing, respectively. The innermost layer containing the largest amount of zirconia, AZ0.6, was thinner than the other layers. The standard deviation of the layers' thicknesses is relatively high. This can be explained by the non-uniform physical properties of the porous mould, such as moisture soaking and ageing. The measured strengths for the small-sized sample were 317 MPa (bottom alumina layer loaded in tension) and 378 MPa (top alumina layer loaded in tension). The average strength value is comparable to the value of homogeneous slip-cast alumina reported in literature 11. The slight strength enhancement can be attributed to the compressive thermal residual stresses in the alumina layers of the five-layered composite resulting from the cooling process because of the different thermal expansion coefficients of the different layers. However, the expected strength enhancement should be higher than that observed experimentally. One of the possible explanations for this discrepancy is the problems of processing, such as non-uniform draining of water from the porous mould, and surface effects, such as trapped air bubbles, which were not released with grinding and polishing of the surface. In the small-sized composite no tunnelling cracks were observed.

In contrast, the large-sized sample exhibited tunnelling cracks, even though the fabrication process was similar. The cracks are spread from the innermost layer out toward the surface alumina layers, but they do not extend to the very surface (Fig. 1) because of the compressive stresses in the outer alumina surface layers. We assumed that the different behaviours of the small- and large-sized samples in terms of the tunnelling cracks were mainly a consequence of the different thicknesses of the innermost layer. In addition, the phenomenon of varying the shrinkage during sintering could create extra stresses, which could also be the reason for the appearance of tunnelling cracks.[12] In any case, the tunnelling cracks strongly decrease the strength of the large-sized samples in comparison to the small-sized samples, as shown in Table 3.

The strength value of the large-sized composite depends on the undamaged parts of the alumina layers (the thickness of the alumina layers from the end of the tunnelling crack to the surface of the composite), so when the thickness of the undamaged layer

Table 1
Layer composition and thickness of the small- and large-sized composites

Layer composition	Thicknesses			
	Small-sized		Large-sized	
	d_i (μm)	d_i/D (%)	d_i (μm)	d_i/D (%)
A (top)[a]	507 ± 102	19.34	707 ± 41	20.55
AZ0.8	675 ± 73	25.74	646 ± 130	18.77
AZ0.6	341 ± 52	13.00	488 ± 104	14.18
AZ0.8	410 ± 77	15.64	712 ± 66	20.69
A (bottom)[b]	689 ± 72	26.28	888 ± 121	25.81

Thicknesses d_i are written in absolute values and relative to the thickness D of the composite.
[a] Top: the alumina layer exposed to the atmosphere.
[b] Bottom: the alumina layer at the porous mould.

Table 2
Material parameters for A, AZ0.8 and AZ0.6 layer compositions: elastic modulus E, Poisson's number ν and linear thermal expansion coefficient α

Layer composition	E (GPa)	ν	α (10^{-6} K^{-1})
A	397	0.238	8.43
AZ0.8	356	0.255	8.85
AZ0.6	315	0.273	9.34

The data were taken from Ref. 7.

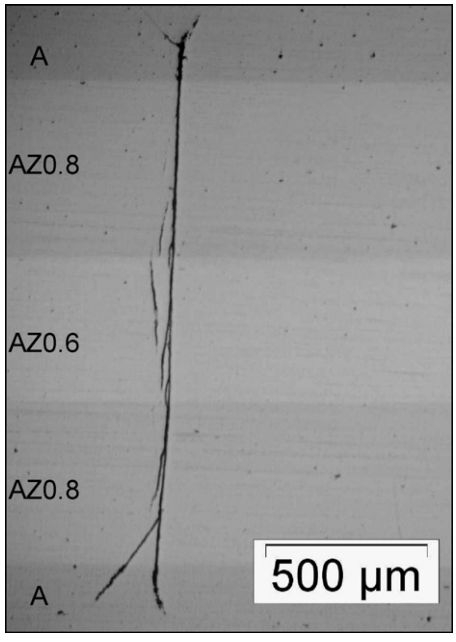

Fig. 1. Optical micrograph of the polished surface of a tunnelling crack in the large-sized sample, showing side (parallel) branching and bifurcations.

Table 3
The thickness of damaged and undamaged parts of outer alumina layers in the large-sized sample and the corresponding bending strength

Layer loaded in tension	Alumina layer (μm)		Strength (MPa)
	Damaged[a]	Undamaged[b]	
Top[c]	149 ± 61	558 ± 75	76 ± 13
Bottom[c]	137 ± 75	751 ± 141	115 ± 14

[a] Part of the crack length extending into the outermost layer.
[b] Distance from the end of the tunnelling crack to the surface.
[c] See the comment below Table 1.

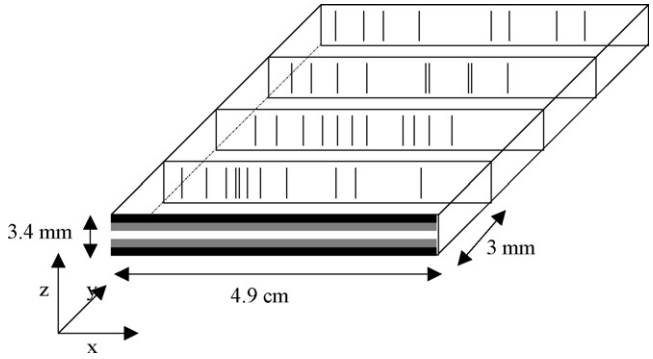

Fig. 3. The experimentally obtained positions of the tunnelling cracks through the depth of the large-sized sample. The number of tunnelling cracks from front to back: 11, 11, 9 and 8. The coordinate system representing the orientation of the layered sample is also shown.

was larger, a higher strength was measured, although the part of the length of the tunnelling cracks extending into the alumina layer was not changed.

Further examination of the large-sized composites cut perpendicular to the layers revealed a crack bifurcation in some cases (Fig. 1). SEM microscopy was used to study the fractured surface around the tunnelling cracks at the section in the innermost layer where we expected their origin to be (Fig. 2). Fig. 2a shows predominantly intergranular fracture with some of its grains fractured in the transgranular mode. The thickness of the tunnelling crack is 0.7 μm, as shown in Fig. 2b. An SEM examination of the fracture surfaces along the crack did not reveal the origin of the crack. However, based on the fact that the fracture is partly transgranular, we assume that the cracks initiated during cooling.

The tunnelling cracks in the large-sized composite were observed with an optical microscope. The number of tunnelling cracks and the inter-crack distances differed from one cross-section to another, as presented in Fig. 3. This fact suggested that the individual cracks merged or split through the depth of the composite. To check this assumption, the top surface of the composite was ground to remove the alumina layer, so that the tunnelling cracks were visible from the top view, and the so-prepared surface was polished. The top view of the tunnelling cracks in the large-sized composite, which is parallel to the layers, reveals the crack splitting (see Fig. 4).

The composites were cut in just one lateral direction. But because of the symmetry of the composite in both lateral directions, we expect a similar picture in the perpendicular direction. As seen from Fig. 4b, neither of the lateral directions is privileged.

3.1. Analytical examination

We checked theoretically the appearance/non-appearance of tunnelling cracks for the two cases of the five-layered composites considered above (the small- and large-sized samples). It is important to note that we are not studying the appearance of cracks due to applied stresses (for instance in the bending test), but we are interested in the cracks that appear during the material processing. The appearance of tunnelling cracks in the sample depends on the compositions and thicknesses of the individual layers. We neglected the edge effects and assumed a uniform, biaxial stress within each layer, which allows for an analytical evaluation of the stresses in the composite. We followed the approach given in Ref. 7, which was developed for symmetrical three-layered composites, although we generalized the formulas for the application to non-symmetrical multilayer composites. Because of the different thermal expansion coefficients of the different layers after sintering, residual thermal stresses are developed in the material after cooling to room temperature. These stresses can be calculated if the values for ΔT, α_i, E_i, ν_i (Table 2) and d_i are known. Here, the index i labels the different layers, ΔT is the temperature span upon cooling the samples, α_i

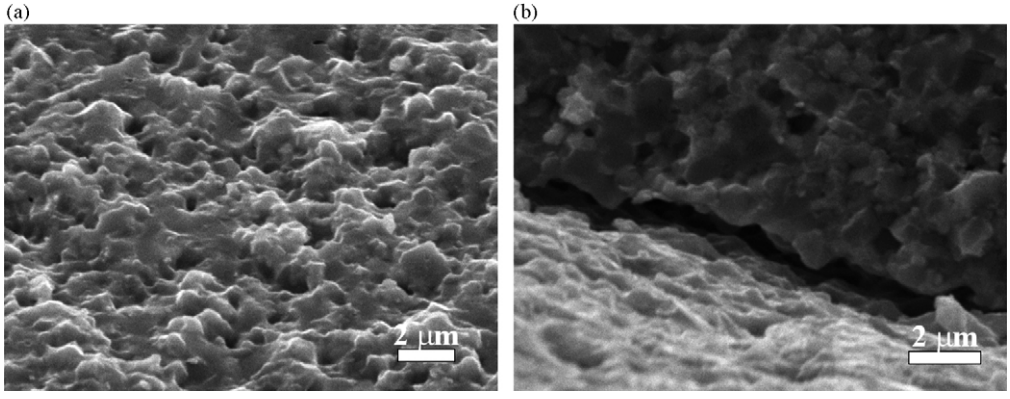

Fig. 2. SEM micrographs of the fracture surface surrounding the tunnelling crack: (a) fracture surfaces and (b) the width of the tunnelling crack. The micrograph is taken from the section of the crack in Fig. 1 in the innermost layer.

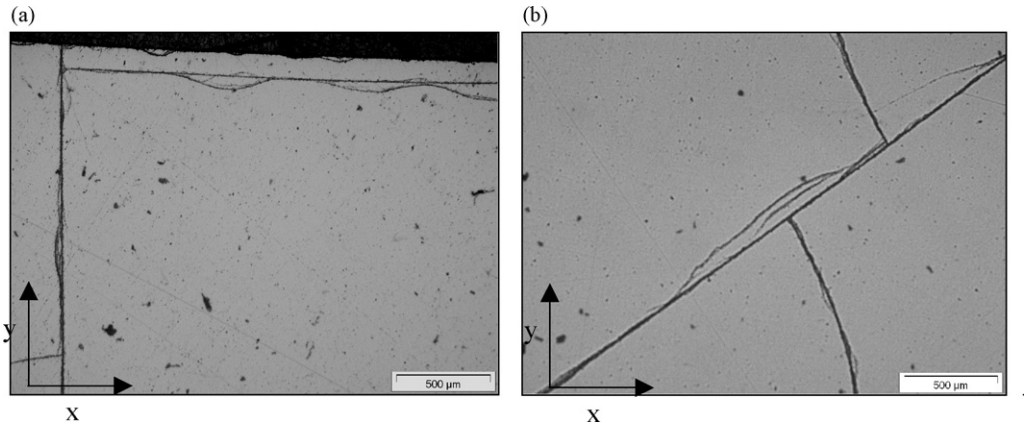

Fig. 4. Top view of the tunnelling cracks in the large-sized composite after the removal of the top surface alumina layer at two different places: (a) near the lateral sample edge and (b) away from the edge. The layers are stacked one above another, so that the top view shows the interior of one of the inner AZ layers.

are the thermal expansion coefficients (averaged over the whole temperature interval), E_i are the elastic moduli, ν_i are the Poisson's ratios and d_i are the thicknesses of the individual layers. For ΔT we chose the value 1300 °C, as suggested in Ref. 7, for a typical sintering condition. The authors in Ref. 7 actually studied the system of alumina and cubic zirconia, but in the literature it was shown that the above-mentioned parameters are similar for the alumina and the tetragonal stabilized zirconia.[3] It should be pointed out that the lateral dimensions of the sample play no role in the calculation. The composition of the layers is such as to obtain lower thermal expansion coefficients for outer layers in comparison to the inner layers, causing compressive and tensile residual stresses in the outer and inner layers, respectively. This choice is appropriate for enhancing the bending strength of the composite. In the layers under tensile stress, tunnelling cracks can occur and propagate, especially in the innermost ($i = 3$) layer, provided that the stress–intensity factor[7,13]

$$K_3 = \sqrt{\frac{2d_3}{\pi}}\sigma_3 \tag{1}$$

exceeds the fracture toughness K_{IC} of the (innermost) layer. Actually, there are two steps in the development of long tunnelling cracks: crack initiation and steady-state growth of the crack through the middle layer. In the crack-initiation process the crack is assumed to be penny shaped, with its diameter being smaller than the thickness of the middle layer. Eq. (1) describes the threshold condition where the diameter of the penny-shaped crack becomes equal to the middle-layer thickness. In this stage, in the case of a three-layered composite with outer layers under compression, the penny-shaped crack starts to extend more easily inside the middle layer and becomes elongated. There is another condition for the steady-state propagation of the tunnelling crack, when its length becomes much greater than the thickness of the middle layer.[13] But it has been shown that once the condition for crack initiation is fulfilled the crack always develops into a long tunnelling crack.

The values of the material parameters for the different compositions are obtained by using fitting parameters from literature.[7,14,15] For instance, we take a fracture toughness of 6.15 MPa m$^{1/2}$ for AZ0.6.[15] For this composition we got a similar result, 6.3 MPa m$^{1/2}$, with the Vickers indentation technique.[11] For experimentally obtained samples (columns "Exp." in Tables 4 and 5) we calculated the following values for the residual thermal tensile stress, and based on Eq. (1), the corresponding stress–intensity factor in the layer AZ0.6, respectively: $\sigma_3 = 350$ MPa, $K_3 = 6.16$ MPa m$^{1/2}$ for the large-sized sample, and $\sigma_3 = 350$ MPa, $K_3 = 5.16$ MPa m$^{1/2}$ for small-

Table 4
Calculation of the stress–intensity factor in the innermost layer for the large-sized sample, with varying layer thicknesses (changed thicknesses with respect to experimental values are written in bold)

Sample composition	d (μm)			
	Exp.[a]	Ch1[b]	Ch2[b]	Ch3[b]
A	707	707	707	**353**
AZ0.8	646	646	**969**	646
AZ0.6	488	**244**	488	488
AZ0.8	712	712	**1068**	712
A	888	888	888	**444**
Total thickness	3441	3323	4935	2963
K_3 (MPa m$^{1/2}$)	6.16	4.65	5.93	5.29

[a] Experimental values of layer thicknesses.
[b] Examples of changed thicknesses (the thicknesses d_2 in d_4 in column Ch2 and the thicknesses d_1 and d_5 in column Ch3 are changed proportionally).

Table 5
Calculation of the critical thicknesses for the appearance of tunnelling cracks in the small-sized sample (varying bold thicknesses)

Sample composition	d (μm)			
	Exp.[a]	Cal1[b]	Cal2[b]	Cal3[b]
A	507	507	507	**1369**
AZ0.8	675	675	–[c]	675
AZ0.6	341	**558**	341	341
AZ0.8	410	410	–[c]	410
A	689	689	689	**1860**
Total thickness	2622	2836	–	4655

[a] Experimental values of layer thicknesses.
[b] Calculated marginal thicknesses for crack appearance (the thicknesses d_1 and d_5 in column Cal3 are changed proportionally).
[c] With decreasing the thicknesses of AZ0.8 layers toward zero value, we do not reach the threshold.

sized sample. Thus, the calculated values of the stress–intensity factor compared to the fracture toughness of the AZ0.6 confirm the observation that the cracks are present in the large-sized sample, but not in the small-sized one. For large-sized samples, where the experimental values of the layer thicknesses are just on the margin of crack appearance we can prevent cracks in different ways, for instance, if the thickness of the innermost layer is reduced. Table 4 shows the calculated values of K_3 for comparison. We also made calculations to show how the thicknesses of the individual layers for smaller samples should be changed so that we come to the margin of the condition for the appearance of tunnelling cracks: $K = K_{IC}$ (in the middle layer). The results are shown in Table 5. For instance, the middle layer should be thicker: 558 μm instead of 341 μm. We see that the experimental middle-layer thickness for the small-sized sample is well below the threshold. It should also be noted that although in the set of investigated layer thicknesses the tensile stresses appear in the second and fourth layers as well as in the inner layer, the stress–intensity factor in the second and fourth layers is well below the fracture toughness for AZ0.8. It should also be noted that the data for the material parameters from the literature should be treated with some caution, because the data differ according to the different starting powders (i.e., how much yttria is in the stabilized zirconia), microstructure, porosity, etc. But, for instance, in Ref. 3, the values of most of the material parameters are similar to the ones used in our calculations.

4. Conclusions

Tunnelling cracks were observed in a large-sized five-layered A/AZ0.8/AZ0.6/AZ0.8/A composite. In contrast, in a small-sized composite with the same sequence and composition of individual layers no such defects were present. The geometrical position of the tunnelling cracks through the composite revealed the non-uniform position of the cracks, and this observation was confirmed using a top view of the tunnelling cracks in the composite where many crack splits were observed. The SEM analysis of the fracture surface surrounding the crack revealed that the fracture is partly transgranular. The bending strength of such a composite was low (76 MPa and 115 MPa) compared to a composite without tunnelling cracks (317 MPa and 378 MPa). An analytical examination confirmed the appearance of tunnelling cracks in the large-sized sample and no cracks in the small-sized sample. A non-cracked large-sized sample could be fabricated when, for instance, the thickness of the inner AZ0.6 layer was decreased. In contrast, in the small-sized composite the tunnelling cracks would appear if, for instance, we significantly increased the thickness of the AZ0.6 layer.

References

1. Sergo, V., Room-temperature aging of laminate composites of alumina/3-mol% yttria-stabilized tetragonal zirconia polycrystals. *J. Am. Ceram. Soc.*, 2004, **87**(2), 247–253.
2. Oechsner, M., Hillman, C. and Lange, F. F., Crack bifurcation in laminar ceramic composites. *J. Am. Ceram. Soc.*, 1996, **79**(7), 1834–1838.
3. Hillman, C., Suo, Z. and Lange, F. F., Cracking of laminates subjected to biaxial tensile stresses. *J. Am. Ceram. Soc.*, 1996, **79**(8), 2127–2133.
4. Sergo, V., Lipkin, D. M., De Portu, G. and Clarke, D. R., Edge stresses in alumina/zirconia laminates. *J. Am. Ceram. Soc.*, 1997, **80**(7), 1633–1638.
5. Ho, S., Hillman, C., Lange, F. F. and Suo, Z., Surface cracking in layers under biaxial, residual compressive stress. *J. Am. Ceram. Soc.*, 1995, **78**(9), 2353–2359.
6. Rao, M. P. and Lange, F. F., Factors affecting treshold strength in laminar ceramics containing thin compressive layers. *J. Am. Ceram. Soc.*, 2002, **85**(5), 1222–1228.
7. Barnett-Ritcey, D. D. and Nicholson, P. S., Failure prediction maps for a model Al_2O_3|c-ZrO_2/Al_2O_3|Al_2O_3 brittle polycrystalline trilayer composite. *J. Am. Ceram. Soc.*, 2003, **86**(1), 121–128.
8. Tomaszewski, H., Residual stresses in layered ceramic composites. *J. Eur. Ceram. Soc.*, 1999, **19**, 1329–1331.
9. De Portu, G. and Micele, L., Characterization of tunneling cracks in Al_2O_3/Al_2O_3 + 3Y-TZP multilayered composites by Raman and fluorescence piezo-spectroscopy. *J. Mater. Sci.*, 2005, **40**, 1505–1508.
10. Reed, J. S., *Principles of Ceramics Processing*. John Wiley and Sons, New York, 1995, pp. 492–503.
11. Beranič, S., Novak, S., Kosmač, T., Richter, H. G. and Hecht-Mijic, S., The preparation and properties of functionally graded alumina/zirconia-toughened alumina (ZTA) ceramics for biomedical applications. *Key Eng. Mater.*, 2005, **290**, 348–352.
12. Novak, S. and Beranič, S., Densification of step-graded Al_2O_3–Al_2O_3–ZrO_2 composites. *Mater. Sci. Forum*, 2005, **492–493**, 207–212.
13. Ho, S. and Suo, Z., Tunneling cracks in constrained layers. *J. Appl. Mech.*, 1993, **60**(12), 890–894.
14. Tsukuma, K., Ueda, K. and Shimada, M., Strength and fracture toughness of isostatically hot-pressed composites of Al_2O_3 and Y_2O_3-partially-stabilized ZrO_2. *J. Am. Ceram. Soc.*, 1985, **68**(1), C-4–C-5.
15. Claussen, N., Strengthening strategies for ZrO_2-toughened ceramics at high temperatures. *Mater. Sci. Eng.*, 1985, **71**, 23–38.